



## A versatile miniature bioreactor and its application to bioelectrochemistry studies

A. Kloke<sup>a</sup>, S. Rubenwolf<sup>a</sup>, C. Bücking<sup>b</sup>, J. Gescher<sup>b</sup>, S. Kerzenmacher<sup>a,\*</sup>, R. Zengerle<sup>a,c</sup>, F. von Stetten<sup>a</sup>

<sup>a</sup> Laboratory for MEMS Applications, Department of Microsystems Engineering - IMTEK, University of Freiburg, Georges-Koehler-Allee 106, 79110 Freiburg, Germany

<sup>b</sup> Institute for Biology II, University of Freiburg, Schänzlestrasse 1, 79104 Freiburg, Germany

<sup>c</sup> Centre for Biological Signalling Studies (bioss), Albert-Ludwigs-Universität Freiburg, Germany

### ARTICLE INFO

#### Article history:

Received 23 September 2009

Received in revised form 16 March 2010

Accepted 14 April 2010

Available online 21 April 2010

#### Keywords:

Modular miniature bioreactor

Experimental setup for bioelectrochemistry

Bioelectrochemical testing

Biofuel cell electrode characterization

### ABSTRACT

Often, reproducible investigations on bio-microsystems essentially require a flexible but well-defined experimental setup, which in its features corresponds to a bioreactor. We therefore developed a miniature bioreactor with a volume in the range of a few millilitre that is assembled by alternate stacking of individual polycarbonate elements and silicone gaskets. All the necessary supply pipes are incorporated as bore holes or cavities within the individual elements. Their combination allows for a bioreactor assembly that is easily adaptable in size and functionality to experimental demands. It allows for controlling oxygen transfer as well as the monitoring of dissolved oxygen concentration and pH-value. The system provides access for media exchange or sterile sampling. A mass transfer coefficient for oxygen ( $k_L a$ ) of  $4.3 \times 10^{-3} \text{ s}^{-1}$  at a flow rate of only  $15 \text{ ml min}^{-1}$  and a mixing time of 1.5 s at a flow rate of  $11 \text{ ml min}^{-1}$  were observed for the modular bioreactor. Single reactor chambers can be interconnected via ion-conductive membranes to form a two-chamber test setup for investigations on electrochemical systems such as fuel cells or sensors. The versatile applicability of this modular and flexible bioreactor was demonstrated by recording a growth curve of *Escherichia coli* (including monitoring of pH and oxygen) saturation, and also as by two bioelectrochemical experiments. In the first electrochemical experiment the use of the bioreactor enabled a direct comparison of electrode materials for a laccase-catalyzed oxygen reduction electrode. In a second experiment, the bioreactor was utilized to characterize the influence of outer membrane cytochromes on the performance of *Shewanella oneidensis* in a microbial fuel cell.

© 2010 Elsevier B.V. All rights reserved.

### 1. Introduction

Bioelectrochemistry includes a variety of research activities in which biological systems are investigated or exploited by electrochemical means. These activities include fundamental studies on electron transfer related phenomena in biology (Dronov et al., 2008; Kim et al., 2004) as well as applications such as electrochemical biosensors (Murphy, 2006; Wang, 2008) and biofuel cells (Bullen et al., 2006; Davis and Higson, 2007; Kerzenmacher et al., 2008). Due to its close relationship to other disciplines,

upcoming developments such as nanoparticles and self-assembly techniques in materials research also revolutionize materials and concepts used in bioelectrochemistry (Chen et al., 2007; Fu et al., 2009).

For keeping track of such rapid developments it is important to be able to comparably investigate materials, technologies and methods new to bioelectrochemistry. In literature, often very simple tentative testing setups are applied, for example constructed from standard laboratory components such as medium bottles (Ren et al., 2007; Logan et al., 2006; Min et al., 2005). These can be used for different microorganisms, are fast to setup, but mostly allow for large volumes only. In general, parallel operation and integration of parameter control systems is possible, but lacks handling comfort and accuracy if only implemented in a tentative manner. The importance of suitable testing cells has recently been indicated by several authors (Gil et al., 2003; Kim et al., 2007; Pham et al., 2006). For instance, they underlined the risk of insufficient oxygen transfer and high internal resistances in improper testing setups because this way the testing cell can artificially limit fuel cell performance. In contrast, more elaborate and tailored testing cell implementations provide more features and controllability, but in most cases

\* Corresponding author at: Laboratory for MEMS Applications, Department of Microsystems Engineering - IMTEK, University of Freiburg, Georges-Koehler-Allee 103, 79110 Freiburg, Germany. Tel.: +49 761 203 7328; fax: +49 761 203 7322.

E-mail addresses: [arne.kloke@imtek.uni-freiburg.de](mailto:arne.kloke@imtek.uni-freiburg.de) (A. Kloke), [stefanie.rubenwolf@imtek.uni-freiburg.de](mailto:stefanie.rubenwolf@imtek.uni-freiburg.de) (S. Rubenwolf), [clemens.buecking@biologie.uni-freiburg.de](mailto:clemens.buecking@biologie.uni-freiburg.de) (C. Bücking), [johannes.gescher@biologie.uni-freiburg.de](mailto:johannes.gescher@biologie.uni-freiburg.de) (J. Gescher), [kerzenma@imtek.uni-freiburg.de](mailto:kerzenma@imtek.uni-freiburg.de) (S. Kerzenmacher), [zengerle@imtek.uni-freiburg.de](mailto:zengerle@imtek.uni-freiburg.de) (R. Zengerle), [vstetten@imtek.uni-freiburg.de](mailto:vstetten@imtek.uni-freiburg.de) (F. von Stetten).

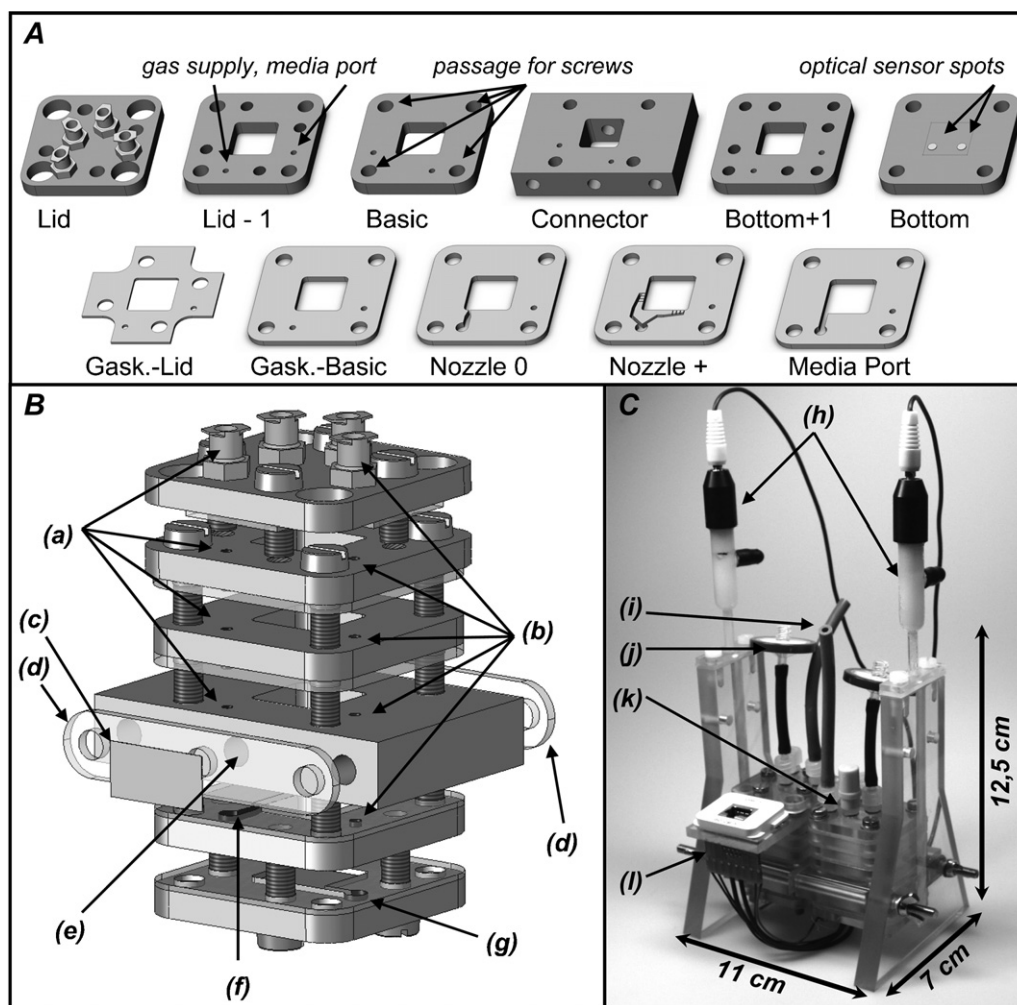


**Fig. 1.** Miniature bioreactor construction kit. (A) Detailed views of the single elements and gaskets used for the miniature bioreactor assembly. The transparent bottom element is equipped with two sensor spots for measuring pH-value and  $O_2$ -concentration. (B) Exploded view of an exemplary miniature bioreactor assembled from the construction kit. The shown bioreactor contains a (a) gas supply channel, (b) access channel for media exchange, (c) ion conductive membrane pressed between two neighboring bioreactors and according gaskets (d), (e) channel for interconnection of neighboring bioreactors, (f) gas nozzle and (g) media port. Luer-lock plugs are used for easy connections at the lid. In the shown assembly the reaction chamber has a volume of 8 ml. (C) Photograph of a dedicated assembly for electrochemical experiments consisting out of separate anode and cathode compartments and two reference electrodes (h) placed into the flanking supports. Connections for (i) gas inlet, (j) gas outlet, (k) sterile sampling and media exchange are provided at the lids. An RJ-45 insert (l) is used to collect the electrical connections of the electrodes.

they consist of a rigid reactor designed to meet a specific problem, and can therefore not easily be adjusted to changing demands (Brunel et al., 2007; Logan et al., 2006). Such systems enable operation at volumes of only a few millilitre (Ringeisen et al., 2006) or even a few microlitre (Qian et al., 2009).

In biotechnological process engineering miniature bioreactors with volumes of 0.1–100 ml are currently used intensively as test reactors before finally large scale production reactors are implemented (Betts and Baganz, 2006; Kumar et al., 2004). In particular bubble column reactors represent a promising concept for the use in bioelectrochemistry, because they feature simple handling and operation at low technical effort, combined with the advantage of growing microorganisms in a controllable environment (Kantarci et al., 2005).

Here we suggest a novel miniature bioreactor construction system with a volume of a few millilitre that is adjustable to experimental demands, allows for reproducible investigations in a controlled and sterile environment, and can thus be used to implement a variety of bioelectrochemical and biotechnological studies.

This modular miniature bioreactor is assembled from single elements to form a bubble column reactor featuring integrated gas

ports, sensors, and the possibility for sterile sampling. Its properties such as size, oxygen transfer coefficient and functionality can be adjusted by selection, number and sequence of the assembled elements. Whereas single reactor columns qualify for the use as stand-alone bioreactors, an interconnected two-column setup is intended for bioelectrochemical investigations with individual compartments for anode and cathode. Here separate reference electrodes are used for anode and cathode to circumvent the influence of the internal resistance on the measurement of electrode potentials. The miniature bioreactors are also designed for operation under anaerobic conditions. This is often required for investigations on microorganisms, for instance to prevent parasitic electron transfer to oxygen in microbial fuel cells (Logan et al., 2006; Pham et al., 2006).

Within this paper firstly the flexible concept of the miniature bioreactor construction system is described in detail (Section 2). Subsequently the methods and materials that were used for the characterization of the novel bioreactor and for demonstration of its applicability to bioelectrochemistry are introduced (Section 3). In the following sections the corresponding experimental results are shown and discussed (Sections 4 and 5).

## 2. Concept of the novel miniature bioreactor construction system

### 2.1. Construction of a miniature bioreactor

The novel modular miniature bioreactor is constructed by alternate stacking of individual polycarbonate elements and silicone gaskets, as shown in Fig. 1(A) and (B). Their central cavities (15 mm × 15 mm in cross-section) form a central reaction chamber. The volume of the central chamber can individually be varied by the number of assembled elements. Typically the volume amounts to a few millilitre. Bore holes in the stacked elements form channels for aeration and media exchange. These channels are connected to the reaction chamber via nozzles and a media exchange port. These functional elements are integrated into silicone gaskets and can be used to vary the reactor's properties such as oxygen transfer by choosing between different gaskets. Four long screws are used to lock the individual parts of the reaction chamber in position. Separate screws are applied to attach the lid and bottom part. At the reactor's lid Luer-lock plugs enable an easy connection of external piping to gas supply and media ports. A transparent bottom element allows for the use of optical sensor spot technology (Wolfbeis, 2004) to measure pH-value or oxygen concentration. Bubbles generated at the gas nozzles support mixing and define the oxygen transfer rate. The media exchange port facilitates access to the reaction chamber for addition or complete exchange of reaction media. If desired, sterile filters can be used to seal off all the openings against microbial contamination. A septum closure at the lid facilitates sterile probe sampling.

### 2.2. Construction of interconnected bioreactor systems

Horizontal bore holes in part "Connector" (see Fig. 1(A)) are intended for interconnection with neighboring reactors, and allow for the construction of larger bioreactor systems. This interconnection can for instance be used for the construction of small-scale chemical synthesizers (Ashmead et al., 1994; Bard, 1996; Snyder et al., 2005). In this case each individual miniature bioreactor would contain one specific physical, chemical or biochemical unit operation required during a multistage synthesis process.

A compact construction of such reactor systems or the parallelized operation of single bioreactors is facilitated by the design of the novel miniature bioreactor because all the connections are either placed on the lid or bottom of the reactor.

### 2.3. Extended setup for electrochemical testing

Fig. 1(C) shows an assembly variation for an electrochemical testing cell consisting of two bioreactor columns and two flanking supports, which each contain one reference electrode. Having separate anode and cathode compartments, this assembly enables the operation of the individual electrodes in separate reaction media without cross-contamination effects. Separate reference electrodes are used to measure the anode and cathode potentials independently, and to circumvent any influence of the ionic resistance of the membrane on the measured potentials. This way also an arbitrary electrode can be used as counter electrode if only a single electrode reaction is to be characterized. Due to the small working volume in the individual compartments, the consequent high concentration of reaction products facilitates their analysis.

### 2.4. Gas supply periphery

Prior to entering the reaction chamber the gases pass a preparation environment consisting out of a gas proportioner, a humidifier column, and a sterile filter. The gas proportioner is used to con-

trol the proportions of oxygen and nitrogen (or other gasses) and thus the composition of the purging gas delivered to the reactor. Furthermore, it enables to set the flow rate and therefore to define the oxygen transfer rate. In a 45 cm high water-filled humidifier column the purging gas gets completely water-saturated, which helps to reduce evaporation of the reaction media inside the reactor. As a last preparation step the inlet gas passes a sterile filter to avoid microbial contamination.

## 3. Materials and methods

### 3.1. Materials

Polycarbonate elements of 5 mm and 12 mm thickness were cut from polycarbonate-sheets (Makrolon<sup>®</sup>, Ketterer + Liebherr, Freiburg, Germany) by water-jet technology and micro-milling, respectively. Silicone rubber gaskets (2 mm thickness, VWR, Bruchsal, Germany) and Viton<sup>®</sup> nozzle elements (1 mm thickness, Lézaud, Marpingen, Germany) were cut with a CO<sub>2</sub>-laser. Silicone tubes as well as Luer-lock connections were purchased from Novodirect (Kehl, Germany). Septum closures were delivered from Greiner Bio-One (Frickenhausen, Germany). Two types of sterile filters were used for the experiments, each having a pore size of 0.2 μm: smaller syringe filters (FP 30/0.2 CA-S, Whatman GmbH, Dassel, Germany) at gas inlet and media exchange ports, and a low pressure loss filter (Midisart 2000, Sartorius AG, Göttingen, Germany) at the gas outlet. Optical sensor systems (Oxy-4 mini and pH-1 mini) and sensor spots by PreSens – Precision Sensing GmbH (Regensburg, Germany) were utilized to monitor oxygen concentration and pH-value. Gas proportioners enabling flow rates up to 814 ml min<sup>-1</sup> were purchased from Analyt-MTC GmbH & Co. KG (9P01/1 with tubes 032-41-ST, Müllheim, Germany) and used to set the oxygen partial pressure of inlet gasses.

### 3.2. Determination of mass transfer coefficient for oxygen and parasitic oxygen permeation

Mass transfer coefficients for oxygen ( $k_L a$ ) were determined at different oxygen flow rates from 0 ml min<sup>-1</sup> to 16 ml min<sup>-1</sup> by the dynamic oxygen method (Linek et al., 1989). Hereto the reaction chamber was purged with nitrogen until an oxygen saturation of less than 0.1% was reached. Subsequently the reactor was aerated with pure oxygen. Gas flow rates were set utilizing a gas proportioner. The experiments were performed in a single miniature bioreactor (as shown in Fig. 1(B)) filled with 7 ml of phosphate buffered saline (PBS tabs pH = 7.4, Invitrogen GmbH, Karlsruhe, Germany). Finally,  $k_L a$  values were extracted by fitting the increase in oxygen saturation to Eq. (1):

$$\frac{dC}{dt} = k_L a (C_{eq} - C) \quad (1)$$

Here  $C$  stands for the dissolved oxygen saturation (in %) inside the reactor measured at time  $t$ , and  $C_{eq}$  is the corresponding equilibrium value (100% oxygen saturation during our experiments).

Similar to the determination of the mass transfer coefficient of oxygen the permeability of the setup towards oxygen was investigated. The reactor was purged with nitrogen until an oxygen saturation of lower than 0.1% was achieved. Subsequently the gas flow was stopped and a permeation rate  $k_{perm}$  was extracted from the exponential increase in oxygen saturation.

### 3.3. Characterization of mixing

To characterize mixing behavior, 0.15 ml of ink was introduced into the miniature bioreactor (filled with 7 ml of water) through the reactor's media port. This experiment has been conducted firstly

at an air flow rate of  $11 \text{ ml min}^{-1}$ , and subsequently without any bubbling. Images of the temporal evolution of the ink distribution inside the reaction chamber were taken through the bottom part using a  $\mu\text{Eye 2230}$  camera (IDS Imaging Development Systems, Obersulm, Germany) mounted onto a microscope (Leica MZ6, Wetzlar, Germany). Subsequently, ink distribution was quantitatively evaluated for selected subareas ( $200 \times 200$  pixels) of the taken images using Adobe Photoshop (Version 9.0). Here the decrease in luminance intensity observed from histograms was utilized as an indicator for the increasing presence of ink and thus mixing progress.

### 3.4. *E. coli* cultivation

LB-medium (7 ml, Sigma–Aldrich, Munich, Germany) with  $50 \mu\text{g ml}^{-1}$  Ampicillin (Roche, Germany) and 0.2 ml over-night culture (optical density at 650 nm: 1.59) of *E. coli* JM109 with control vector pGEM-3Z (both obtained from Promega, Mannheim, Germany) were inoculated and cultivated at  $37^\circ\text{C}$  under aeration with pure air. Samples of 0.15 ml were taken each 20–60 min and analyzed for their optical density at 650 nm (UV300, Unicam Instruments, UK). Oxygen saturation and pH-value were continuously recorded during fermentation using optical sensor spots (PreSens – Precision Sensing GmbH, Regensburg, Germany)

### 3.5. Characterization of electrode materials for an enzymatic laccase cathode

Electrodes made of graphite felt ( $1.54 \text{ cm}^3$ , Alfa Aesar, Karlsruhe, Germany), HOPG ( $0.29 \text{ cm}^3$  highly ordered pyrolytic graphite, SPI supplies, USA) or porous carbon tubes ( $0.45 \text{ cm}^3$ , Novasep, Epone, France) were glued to platinum wires (Chempur, Karlsruhe, Germany) using conductive carbon cement (Leit-C, Plano, Wetzlar, Germany) and subsequently mounted above the bottom part in the cathode compartment in the bioreactor assembly shown in Fig. 1(C). Laccase from *Trametes versicolor* (20 U, Sigma–Aldrich, Munich, Germany) was solved in 4 ml of  $0.1 \text{ mol l}^{-1}$  citrate buffer (pH 5, Sigma–Aldrich, Munich, Germany) and introduced into the cathode compartment. Experiments were performed at room temperature while the cathode compartment was continuously purged with air (flow rate  $170 \text{ ml min}^{-1}$ ).

A platinum mesh in citrate buffer served as counter electrode inside the anode compartment. A saturated calomel reference electrode (SCE, KE 11, Sensortechnik Meinsberg GmbH, Ziegra-Knobelsdorf, Germany) was placed in each flanking element. The individual compartments and flanking elements were separated from each other by a cation exchange membrane (Fumapem F-950®, FuMA-Tech, St. Ingbert, Germany).

To conduct load curve experiments the electrical testing environment described elsewhere (Kerzenmacher et al., 2009) was used. This system is able to set constant galvanostatic loads using stimulus generators (STG2008, Multichannel Systems, Reutlingen, Germany) and to simultaneously record electrode potentials with a Keithley 2700 data acquisition system (Keithley, Gemering, Germany). To record data for galvanostatic load curves electrode potentials were measured against the reference electrodes at stepwisely increased galvanostatic loads between cathode and the counter electrode. This galvanostatic load was increased by  $5 \mu\text{A}$  every hour and the last value recorded before the load increment served for load curve construction.

### 3.6. Characterization of electron transfer in *Shewanella oneidensis*

The miniature bioreactor was assembled as shown in Fig. 1(C). A cubic graphite felt ( $1.64 \text{ cm}^3$ ) was used as electrode, electrically

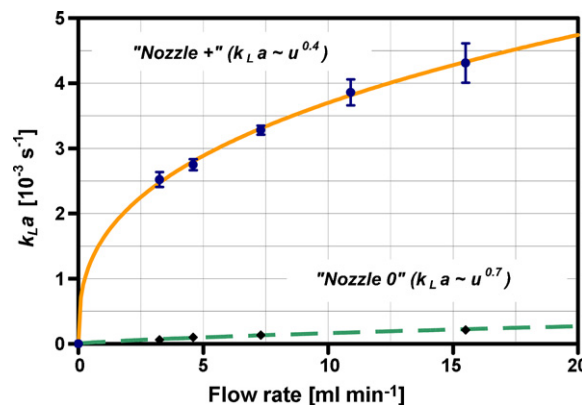


Fig. 2. Comparison of two different nozzles concerning their mass transfer coefficients for oxygen ( $k_L a$ ) in dependence of the applied oxygen flow rate. Data was recorded for a single miniature bioreactor compartment filled with 7 ml PBS. Error bars correspond to the standard deviations of fitted  $k_L a$  values obtained by the dynamic oxygen method.

connected in the same way as described for the enzymatic cathodes. A platinum mesh in the cathode compartment was used as counter electrode. Nafion® membranes (Nafion-117, Quintech, Göppingen, Germany) were used to separate the single compartments.

*S. oneidensis* cells were cultivated under anaerobic conditions in minimal medium (Gescher et al., 2008) containing  $0.05 \text{ mol l}^{-1}$  sodium lactate and  $0.1 \text{ mol l}^{-1}$  fumarate. Cells were washed in minimal medium without fumarate and lactate and 12 ml of a cell suspension with an optical density of 0.025 at a wavelength of 600 nm was applied to the anode compartment. During experiments the anode compartment was constantly purged with nitrogen. To start the experiment, sodium lactate was added as electron donor and carbon source to reach a final concentration of  $0.05 \text{ mol l}^{-1}$ .

Load curve experiments were in general conducted in the same way as for the enzymatic cathodes (see Section 3.5) with the exception that the load current was increased in steps of  $5 \mu\text{A}$  once the electrode potential stabilized to values within a limit of  $4 \text{ mV h}^{-1}$ . Load curves were constructed accordingly.

## 4. Characterization of the miniature bioreactor

### 4.1. Oxygen transfer

Two different nozzle configurations are compared in Fig. 2 by their mass transfer coefficients for oxygen determined at different volume flow rates. For the configuration “Nozzle +” (Fig. 1(A), nozzle cross-section:  $\sim 200 \mu\text{m} \times 350 \mu\text{m}$ ) generally higher oxygen transfer rates are observed as for configuration “Nozzle 0” (Fig. 1(A), nozzle cross-section:  $\sim 900 \mu\text{m} \times 600 \mu\text{m}$ ): at an oxygen flow of  $15.5 \text{ ml min}^{-1}$  a  $k_L a$  value of  $4.3 \times 10^{-3} \text{ s}^{-1}$  was obtained for “Nozzle +”, and only  $2.1 \times 10^{-4} \text{ s}^{-1}$  for “Nozzle 0”. The better performance of “Nozzle +” is mainly due to the smaller outlet cross-section generating smaller bubbles, resulting in a higher interfacial area and consequently in a faster oxygen transfer (Linek et al., 1989).

For bubble column reactors the mass transfer coefficient for oxygen is usually described by a simple power function of the form  $k_L a(u) \sim u^b$  in dependence of the volume flow rate  $u$  (Doig et al., 2005).  $k_L a$  values obtained for “Nozzle +” show proportionality to  $u^{0.4}$ , while a relation to  $u^{0.7}$  is found for “Nozzle 0”. Due to the smaller exponent, “Nozzle +” shows a relatively lower relative sensitivity towards fluctuations in the gas flow rate as compared to “Nozzle 0”.

Compared to state of the art the achieved  $k_L a$  values for the novel bioreactor at flow rates up to  $15 \text{ ml min}^{-1}$  ( $k_L a = 4.3 \times 10^{-3}$ )

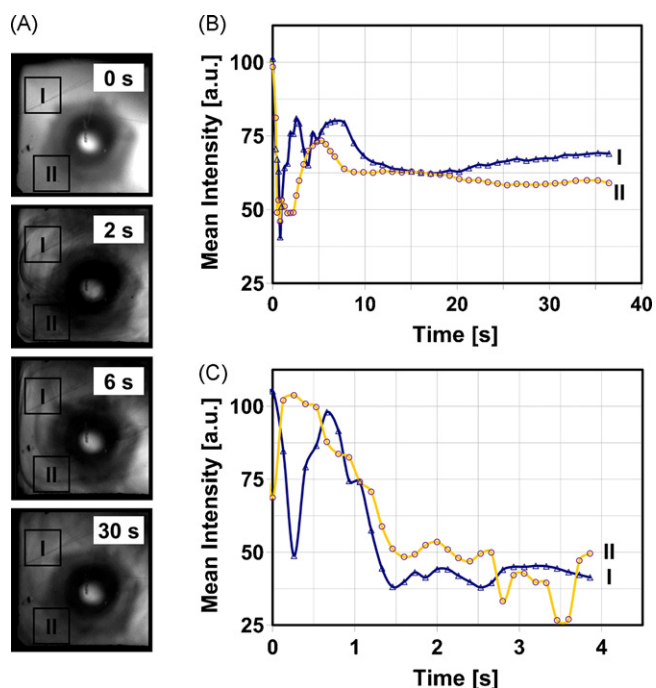


**Fig. 3.** Temporal evolution of luminance decay after addition of ink to a non-agitated bioreactor. (A) Exemplary snapshot of a non-agitated bioreactor chamber (view from underneath). The delineated boxes I/II represent the subareas for which the luminance decay was examined. (B) and (C) show the luminance decay observed in the two arbitrarily selected subareas recorded for a non-agitated (B) and an aerated bioreactor (C, flow velocity  $11 \text{ ml min}^{-1}$ ). Luminance intensity is presented relative to the luminance level before the addition of ink.

are lower than reported for non-modular miniature bioreactors (up to  $6 \times 10^{-2} \text{ s}^{-1}$ ) (Doig et al., 2005). The oxygen transfer coefficient of the novel bioreactor may be increased either by higher flow rates or by changing the nozzle geometry. To obtain oxygen transfer rates of more than  $10^{-2} \text{ s}^{-1}$  with “Nozzle +” a volume flow rate of more than  $160 \text{ ml min}^{-1}$  would be required. Geometrical ways to enhance the oxygen transfer into the bioreactor would be to minimize the nozzle opening, to elongate the path length of bubbles inside the reactor or to increase the number of gas inlets.

#### 4.2. Parasitic oxygen transfer

For anaerobic conditions the miniature bioreactor can be purged with nitrogen to displace oxygen from the reaction chamber. Without nitrogen purging oxygen permeates through the reactor’s walls into the reaction chamber causing an increase in oxygen concentration according to Eq. (1) with a rate constant  $k_{\text{perm}}$  of  $3 \times 10^{-4} \text{ s}^{-1}$ . This means that after nitrogen purging is stopped it lasts 15 min until the oxygen saturation increases from less than 0.1–5%. If a lower permeability is required silicone gaskets could be replaced by other materials such as Viton® which exhibits a by two orders of magnitude lower oxygen permeability (Kjeldsen, 1993).

#### 4.3. Mixing

The mixing behavior of the novel miniature bioreactor is compared for both non-agitated and bubble-driven operation in Fig. 3. This comparison is based on the time required until the ink added to the compartment is homogeneously distributed, indicated by a constant level in luminance intensity. Fig. 3(A) shows exemplary snapshots of a movie taken from underneath the bioreactor during non-agitated operation. In this case non-dispersed streaks were observed throughout the reaction chamber during the first 10 s after the addition of ink. The delineated boxes correspond to the

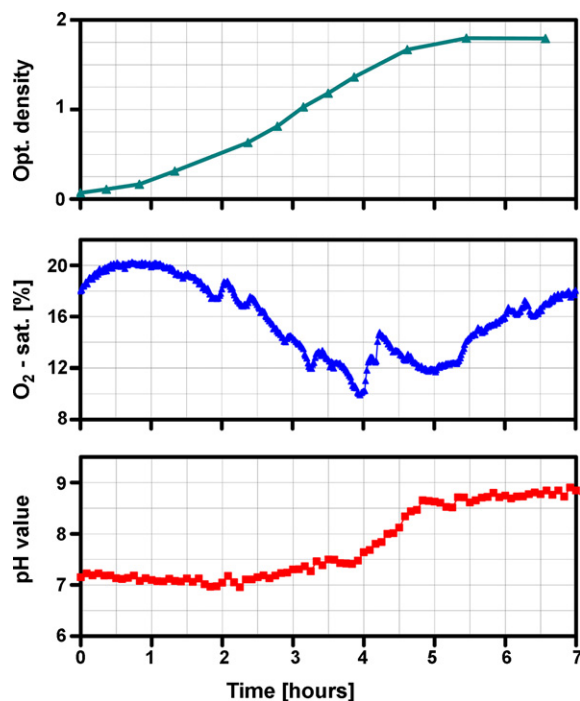


**Fig. 4.** Cultivation of *E. coli*. The figure shows the temporal evolution of optical density, oxygen saturation and pH-value over a period of 7 h. After 4 h the applied flow rate was increased from  $23 \text{ ml min}^{-1}$  to  $38 \text{ ml min}^{-1}$ .

two subareas which were further analyzed by their temporal evolution in luminance intensity. Fig. 3(B) shows the corresponding analysis for the non-agitated case with strong up and downs in luminance intensity during the first 10 s. After 10 s only a slight and slow variation remains in luminance evolution. Single snapshots still show streaks after 30 s. Therefore we have to conclude, that the mixing process is not completed after 30 s.

For bubble-driven mixing (see Fig. 3(C)) luminance analysis shows that mixing is completed after 1.5 s. The later appearing deviations in luminance intensity are caused by the influence of bubbles in the optical pathway and not by streaks of ink. With 1.5 s the observed mixing time is comparable to other miniature bioreactors (Isett et al., 2007).

#### 4.4. Cultivation of *E. coli*

Fig. 4 shows a temporal evolution of biomass concentration, oxygen saturation, and pH-value during *E. coli* – fermentation within an aerated novel miniature bioreactor. The growth of biomass saturates after 6 h at an optical density of 1.79. Oxygen saturation strongly decreases during the growth period and starts to regenerate as soon as the growth rate decreases. The pH-value develops in a similar way as the biomass concentration and increases from 7.1 to 8.8. The observed curve propagations correspond to what is reported for *E. coli* systems in literature (Lee et al., 2006; Doig et al., 2005). After 4 h the applied air flow rate was increased from  $23 \text{ ml min}^{-1}$  to  $38 \text{ ml min}^{-1}$ . This did not lead to a significant change in growth rate of the biomass concentration.

### 5. Bioreactor application in biofuel cell research

#### 5.1. Characterization of electrode materials for an enzymatic laccase cathode

Laccase is a selective catalyst for the reduction of oxygen to water. It is known to adsorb at carbon-based electrodes and to

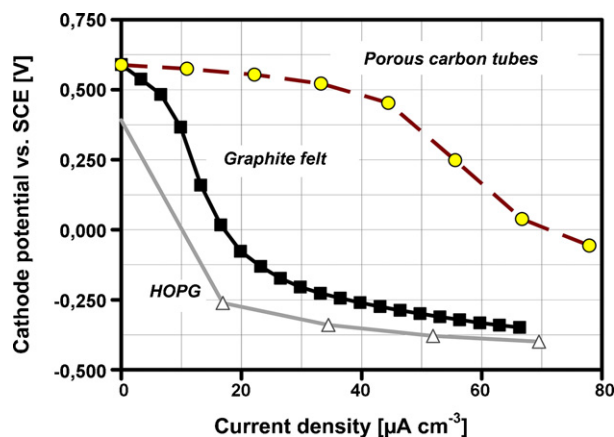


Fig. 5. Comparison of polarization behavior of different carbon-based laccase cathodes. The electrode potential is presented in dependence of the applied current load and normalized by the electrode volume.

exchange electrons with such electrodes without the use of a mediator (direct electron transfer). The performance of a laccase cathode hereby strongly depends on the electrode material. Laccase cathodes are frequently described in literature (Brunel et al., 2007; Habrioux et al., 2007; Kamitaka et al., 2007; Vincent et al., 2005), but in all cases the influence of the electrode material could not clearly be observed because the cathodes were not independently characterized from their counter electrodes.

Using the assembly for electrochemical experiments shown in Fig. 1(C), the cathode potentials under load are compared for laccase adsorbed to different carbon-based materials in Fig. 5 (Rubenwolf et al., 2008, 2010). Compared to the other materials, the most positive cathode potentials under load were observed for porous carbon tubes. These would therefore be the best choice for application in fuel cells, because a more positive cathode potential corresponds to a higher fuel cell voltage. Comparing the different materials in Fig. 5 at a specific potential one finds higher current densities for graphite felt compared to HOPG and for porous carbon tubes compared to graphite felt, indicating a ranking in terms of their charge transfer rate between electrode and enzyme. This ranking corresponds to the increase in volume-normalized surface area of the different materials.

Applying the presented miniature bioreactor we were thus able to systematically compare the performance of different electrode materials for laccase-catalyzed biofuel cell cathodes, without any influence of the used counter electrode (anode). To our best knowledge, similar studies on laccase cathodes have to date not been reported in literature.

## 5.2. Characterization of electron transfer in *S. oneidensis*

*S. oneidensis* MR-1 is a bacterial strain known for its ability to transfer electrons to insoluble terminal electron acceptors such as iron [Fe(III)] or manganese [Mn(III,IV)]. *S. oneidensis* has been widely used as microbial anode in microbial fuel cells (Bretschger et al., 2007; Ringeisen et al., 2006, 2007; Logan, 2009; Biffinger et al., 2007). This outstanding ability requires a mechanism for electron transfer from the inner membrane through the periplasm to the outer membrane. Hereby multiheme c-type cytochromes are known to play a crucial role (Shi et al., 2007). The operation of microbial anodes using gene deletion based variants of the wild type is one applicable method to characterize the influence of individual c-type cytochromes on the ability of electron transfer (Bretschger et al., 2007; Bücking et al., 2010).

Fig. 6 shows galvanostatic load curves for the wild type of *S. oneidensis*, for heat inactivated wild type cells as well as for a deletion

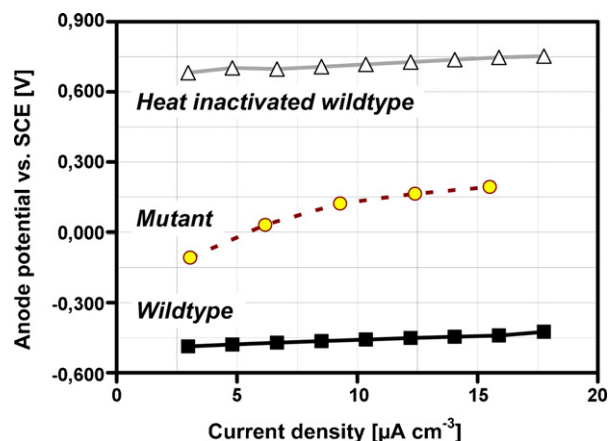


Fig. 6. Galvanostatic load curves recorded for different *S. oneidensis* anodes using wildtype, mutant  $\Delta OMC$  or heat inactivated wildtype as catalyst, respectively. The anode potential is in dependence of an increasing current load. The current density is normalized to the volume of the graphite felt electrode.

mutant in all the annotated outer membrane cytochromes, referred to as  $\Delta OMC$ . The very negative anode potential of the wild type indicates its qualification as an electron donor. The little polarization with increasing current load represents a high transfer rate of electrons from the wildtype to the electrode. For the  $\Delta OMC$  mutant a stronger polarization than for the wildtype is observed. Therefore we can conclude that the removal of outer membrane cytochromes leads to significantly lowered electron transfer rates between organism and electrode. The very positive potential of the heat inactivated wild type indicates the loss of the electron donor properties due to the stopped metabolism.

In this way these bioelectrochemical studies can be used to identify the essential cytochromes for electron transfer in *S. oneidensis*. In a further step the ability for electron transfer could be transferred to other organisms such as *E. coli* by transferring the identified cytochromes.

## 6. Conclusion and outlook

We presented miniature bioreactors assembled from stacked construction system elements as versatile tools for the characterization of diverse bio-microsystems. The novel miniature bioreactors can be customized to specific experimental demands by adjusting choice, number, and sequence of the stacked elements during assembly. Furthermore, they allow for sterile operation and sampling as well as monitoring of pH and oxygen concentration. Since all the access points are placed either at the lid or bottom of the reactor the design supports parallelization at a relatively low space requirement.

For an exemplarily assembled bioreactor a  $k_L a$  value of  $4.3 \cdot 10^{-3} \text{ s}^{-1}$  was observed at an oxygen flow rate of  $15 \text{ ml min}^{-1}$ . This is lower than the values usually reported for non-modular bioreactors. Higher oxygen transfer values are expected to be achievable at higher volume flow rates or with optimized nozzle geometries. With a mixing time of less than 1.5 s at an oxygen volume flow of  $11 \text{ ml min}^{-1}$ , the exemplarily assembled bioreactor shows mixing properties comparable to conventional miniature bioreactors reactors. The versatile applicability of the system has been demonstrated by successful growth of *E. coli* bacteria as well as bioelectrochemical investigations on different types of biofuel cells. Here the suggested bioreactor setup enabled the direct comparison of different carbon-based materials concerning their suitability as electrode for laccase-catalyzed biofuel cell cathodes (independent of anode influences). Furthermore we confirmed the applicability of our miniature bioreactor system for the anaerobic

cultivation of *S. oneidensis*, enabling the study of electron transfer properties of *S. oneidensis* mutants with a reduced number of membrane cytochromes. In this context the controllable bioreactor environment, in particular its defined gas supply and the use of two reference electrodes are essential advantages for reproducible comparative investigations.

With further extensions such as automated sampling, sensors for other parameters or an automated pH-regulation the presented modular setup can be upgraded to a complex but nevertheless flexible platform for automated investigations and process development in bioelectrochemistry or biotechnology. Besides the here shown applications we also suggest this miniature bioreactor as versatile tool for biosensor engineering. In future we plan to use this miniature bioreactor system for analysis of electrochemical reaction products and cytotoxicity tests of implantable electrodes.

## Acknowledgements

Financial support by the German Research Association (DFG) through the PhD program “Micro Energy Harvesting” (GRK 1322) and the German Ministry of Education and Research (BMBF, Projektträger Jülich) under the program “Bioenergie2021” (grant no. 03SF0382) is gratefully acknowledged. Furthermore we would like to thank Oliver Raab for technical assistance.

## References

- Ashmead, J.W., Blaisdell, C.T., Johnson, M.H., Nyquist, J.K., Perrotto, J.A., Ryley, J.F., 1994. European Patent 0 688 242 B1.
- Bard, A.J., 1996. US Patent 5 580 523.
- Betts, J.I., Baganz, F., 2006. *Microb. Cell Fact.*, 5.
- Biffinger, J.C., Ray, R., Little, B., Ringeisen, B.R., 2007. *Environ. Sci. Technol.* 41 (4), 1444–1449.
- Bretschger, O., Obratsova, A., Sturm, C.A., Chang, I.S., Gorby, Y.A., Reed, S.B., Culley, D.E., Reardon, C.L., Barua, S., Romine, M.F., Zhou, J., Beliaev, A.S., Bouhenni, R., Saffarini, D., Mansfeld, F., Kim, B.H., Fredrickson, J.K., Nealson, K.H., 2007. *Appl. Environ. Microbiol.* 73 (21), 7003–7012.
- Brunel, L., Denele, J., Servat, K., Kokoh, K.B., Jolival, C., Innocent, C., Cretin, M., Rolland, M., Tingry, S., 2007. *Electrochem. Commun.* 9 (2), 331–336.
- Bücking, C., Popp, F., Kerzenmacher, S., Gescher, J., 2010. *FEMS Microbiol. Lett.* 306 (2), 144–151.
- Bullen, R.A., Arnot, T.C., Lakeman, J.B., Walsh, F.C., 2006. *Biosens. Bioelectron.* 21 (11), 2015–2045.
- Chen, D., Wang, G., Li, J.H., 2007. *J. Phys. Chem. C* 111 (6), 2351–2367.
- Davis, F., Higson, S.P.J., 2007. *Biosens. Bioelectron.* 22 (7), 1224–1235.
- Doig, S.D., Diep, A., Baganz, F., 2005. *Biochem. Eng. J.* 23 (2), 97–105.
- Dronov, R., Kurth, D.G., Moehwald, H., Scheller, F.W., Lisdat, F., 2008. *Angew. Chem., Int. Ed.* 47 (16), 3000–3003.
- Fu, Y.C., Li, P.H., Xie, Q.J., Xu, X.H., Lei, L.H., Chen, C., Zou, C., Deng, W.F., Yao, S.Z., 2009. *Adv. Funct. Mater.* 19 (11), 1784–1791.
- Gescher, J.S., Cordova, C.D., Spormann, A.M., 2008. *Mol. Microbiol.* 68 (3), 706–719.
- Gil, G.C., Chang, I.S., Kim, B.H., Kim, M., Jang, J.K., Park, H.S., Kim, H.J., 2003. *Biosens. Bioelectron.* 18 (4), 327–334.
- Habrioux, A., Sibert, E., Servat, K., Vogel, W., Kokoh, K.B., Alonso-Vante, N., 2007. *J. Phys. Chem. B* 111 (34), 10329–10333.
- Isett, K., George, H., Herber, W., Amanullah, A., 2007. *Biotechnol. Bioeng.* 98 (5), 1017–1028.
- Kamitaka, Y., Tsujimura, S., Setoyama, N., Kajino, T., Kano, K., 2007. *Phys. Chem. Chem. Phys.* 9 (15), 1793–1801.
- Kantarci, N., Sibert, F., Ulgen, K.O., 2005. *Process Biochem.* 40 (7), 2263–2283.
- Kerzenmacher, S., Ducrée, J., Zengerle, R., von Stetten, F., 2008. *J. Power Sources* 182 (1), 1–17.
- Kerzenmacher, S., Mutschler, K., Kräling, U., Baumer, H., Ducrée, J., Zengerle, R., von Stetten, F., 2009. *J. Appl. Electrochem.* 39 (9), 1477–1485.
- Kim, B.H., Park, H.S., Kim, H.J., Kim, G.T., Chang, I.S., Lee, J., Phung, N.T., 2004. *Appl. Microbiol. Biotechnol.* 63 (6), 672–681.
- Kim, B.H., Chang, I.S., Gadd, G.M., 2007. *Appl. Microbiol. Biotechnol.* 76 (3), 485–494.
- Kjeldsen, A., 1993. *Water Res.* 27 (1), 121–131.
- Kumar, S., Wittmann, C., Heinzle, E., 2004. *Biotechnol. Lett.* 26 (1), 1–10.
- Lee, H.L.T., Boccuzzi, P., Ram, R.J., Sinskey, A.J., 2006. *Lab Chip* 6 (9), 1229–1235.
- Linek, V., Benes, P., Vaclav, V., 1989. *Chem. Eng. Technol.* 12 (1), 213–217.
- Logan, B.E., 2009. *Nat. Rev. Microbiol.* 7 (5), 375–381.
- Logan, B.E., Hamelers, B., Rozendal, R., Schröder, U., Keller, J., Freguia, S., Aelterman, P., Verstraete, W., Rabaey, K., 2006. *Environ. Sci. Technol.* 40 (17), 5181–5192.
- Min, B., Ramanathan, R., Cheng, S., Logan, B., 2005. *Water Res.* 39, 1675–1686.
- Murphy, L., 2006. *Curr. Opin. Chem. Biol.* 10 (2), 177–184.
- Pham, T.H., Rabaey, K., Aelterman, P., Clauwaert, P., De Schampelaire, L., Boon, N., Verstraete, W., 2006. *Eng. Life Sci.* 6 (3), 285–292.
- Qian, F., Baum, M., Gu, Q., Morse, D.E., 2009. *Lab Chip* 9 (21), 3076–3081.
- Ren, Z.Y., Ward, T.E., Regan, J.M., 2007. *Environ. Sci. Technol.* 41 (13), 4781–4786.
- Ringeisen, B.R., Henderson, E., Wu, P.K., Pietron, J., Ray, R., Little, B., Biffinger, J.C., Jones-Meehan, J.M., 2006. *Environ. Sci. Technol.* 40 (8), 2629–2634.
- Ringeisen, B.R., Ray, R., Little, B., 2007. *J. Power Sources* 165 (2), 591–597.
- Rubewolf, S., Kloke, A., Kerzenmacher, S., Zengerle, R., von Stetten, F., 2008. *Biosensors World Congress, Shanghai, China*, P2.23.
- Rubewolf, S., Strohmeier, O., Kloke, A., Kerzenmacher, S., Zengerle, R., von Stetten, F., 2010. *Biosens. Bioelectron.*, doi:10.1016/j.bios.2010.05.008.
- Shi, L., Squier, T.C., Zachara, J.M., Fredrickson, J.K., 2007. *Mol. Microbiol.* 65 (1), 12–20.
- Snyder, D.A., Noti, C., Seeberger, P.H., Schael, F., Bieber, T., Rimmel, G., Ehrfeld, W., 2005. *Helv. Chim. Acta* 88 (1), 1–9.
- Vincent, K.A., Cracknell, J.A., Lenz, O., Zebger, I., Friedrich, B., Armstrong, F.A., 2005. *Proc. Natl. Acad. Sci. U.S.A.* 102 (47), 16951–16954.
- Wang, J., 2008. *Chem. Rev.* 108 (2), 814–825.
- Wolfbeis, O.S., 2004. *Anal. Chem.* 76 (12), 3269–3283.